Proc. of the 9th Intl. Conf. of Asian Society for Precision Engg. and Nanotechnology (ASPEN 2022)
15–18 November 2022, Singapore. Edited by Nai Mui Ling Sharon and A. Senthil Kumar
doi://10.3850/978-981-18-6021-8_OR-09-0016

Simulation of XYθ-axes servo control for one step motion of piezoelectric walking mechanism by Bang-Bang control and PID control

Eiji Kusui[1], Masato Shiota[1], Ryosuke Kinoshita[1], Rintaro Minegishi[1], Eri Fukuchi[1], Yohei Tsukui[1], Yuta Sunohara[1], and Ohmi Fuchiwaki[1#]

1 Department of Mechanical Engineering, Yokohama National University, 79-1 Tokiwadai Hodogaya-ku, Yokohama, Kanagawa, Japan
, #Corresponding Author / Email: ohmif@ynu.ac.jp, TEL: +81-45-339-3693

KEYWORDS: Piezoelectric actuator, Precise positioning, BangBang control, PID control, walking robot

In this paper, we describe an one step motion's control of piezoelectric walking mechanism. The mechanism walks al ternating fixing of two legs to the floor. When one leg is attached to the surface, and the other slides according to displacements of piezoelectric actuators (PAs). We have firstly tried BangBang control, however non-negligible resi dual deviation remained. Then, we have conducted PID control to eliminate the residual deviations, however the s ettling time became longer than 70ms, which is 7 times larger of required value of 10ms. In this paper, we report the simulation of switching control of PID control and BangBang control to reduce both the settling time and the residual deviation, in which PID control worked for fine position adjustment after rough positioning of BangBang control. We confirmed that the objectives were achieved in the simulations. We concluded that the proposed control method is feasible for the precise and fast positioning for flexible manipulation.

NOMENCLATURE

k_L	Spring constant of piezoelectric actuator (PA) in the direction of expansion and contraction
k_s	Spring constant of PA in the direction in shear direction
c_s	Damping coefficient in shear direction of PA
d_F, d_B, d_{R1}, d_{R2}, d_{L1}, d_{L2}	Forced displacement of each PA
P_{G1}, O_{G1}, x_{G1}, y_{G1}	Displacement vector of the center of the gravity of EM-1, its starting point, x component, y component
e_x, e_y, e_θ	Forced displacements in corresponding axis, linear expression of displacements of 6 PAs.
l_0	Offset displacement of PA

1. Introduction

In recent years, electronic devices such as IoT and wearable devices have been developing remarkably, and the built-in electronic components have been miniaturized accordingly. Demand for micromanipulation technology is increasing to make more complex, smaller devices. Furthermore, precise positioning technology has a wide range of applications such as the manipulation of microscopic cells in the development of medical biology and the classification of microfossils in geology. Precision stages are mainly used, but they need excessive energy, weight, and space, relative to the object being operated.

To solve problems above, we are developing a compact and lightweight precision positioning mechanism for use in confined spaces.

We have studied positioning methods of the mechanisms such as compensation of input voltage of actuators, image FB using a camera, closed-loop sequential control using multiple encoders. However, none of them achieved the required accuracy.

Thus, this paper studies a method to improve the accuracy of the motion within a single step of the piezoelectric walking mechanism. The targeted settling time should be less than 10 [ms] when the robot walks with 100 [Hz] with positioning error of less than 0.1 [μm] for one step motion.

In this report, we describe simulation of switching control of BangBang and PID controls. We also check the validity of the proposed control method with comparison of experimental results of BangBang control and PID control.

2. Configuration of the piezoelectric walking mechanism

Shown in Fig. 1, the mechanism consists of two Y-shaped electromagnetic legs and 6 piezoelectric actuators (PA), those are connected by parallel springs to get simultaneous 6 points' contact on a well-polished ferromagnetic floor.

In Fig.1, each PA is marked F, B, R1, R2, L1, and L2 for distinction.

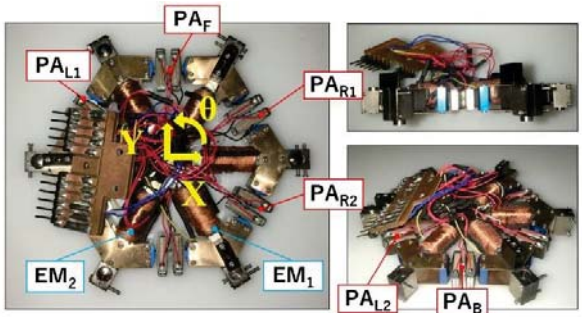

Fig. 1 Configuration of the mechanism

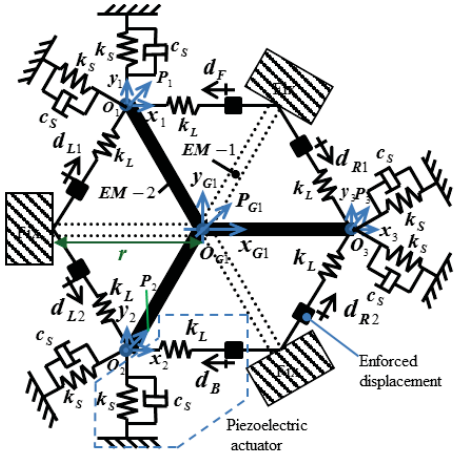

Fig. 2 Mechanical model

Two Y-shaped legs overlap each other vertically to form a regular hexagon and they are separated for not attracting each other. When the mechanism walks, one leg is magnetically attached to the ferromagnetic surface, and the other leg slides according to the expansion and contraction of the PA. Repeating these actions, the mechanism walks repeatedly. By appropriately adjusting the amount of expansion and contraction of each PA, translation, rotation, and revolution around any point are realized holonomically.

3. Mechanical model

Fig. 2 is the mechanical model of the mechanism which its one el ectromagnetic leg (EM-1) is attached to the surface. Another leg (EM -2) slides freely by 6 PAs.

Fig. 3 is a simplified single-axis model of Fig.2, assuming that there is no mutual interference in XYθ axes. e_x, e_y, e_θ is defined as the forced displacement integrating 6 PAs' forced displacements as shown below,

$$\begin{bmatrix} e_x \\ e_y \\ e_\theta \end{bmatrix} = \begin{bmatrix} \frac{k_L}{k_x} & 0 & 0 \\ 0 & \frac{k_L}{k_y} & 0 \\ 0 & 0 & \frac{k_L}{k_\theta} \end{bmatrix} \begin{bmatrix} -1 & -1 & \frac{1}{2} & \frac{1}{2} & \frac{1}{2} & \frac{1}{2} \\ 0 & 0 & \frac{\sqrt{3}}{2} & -\frac{\sqrt{3}}{2} & -\frac{\sqrt{3}}{2} & \frac{\sqrt{3}}{2} \\ \frac{\sqrt{3}}{2} & -\frac{\sqrt{3}}{2} & -\frac{\sqrt{3}}{2} & \frac{\sqrt{3}}{2} & -\frac{\sqrt{3}}{2} & \frac{\sqrt{3}}{2} \end{bmatrix} \begin{bmatrix} d_F - l_0 \\ d_B - l_0 \\ d_{L1} - l_0 \\ d_{L2} - l_0 \\ d_{R1} - l_0 \\ d_{R2} - l_0 \end{bmatrix} \quad (1)$$

The equation of motion for each axis of the movable leg consists of springs, dampers, and forced displacements. We approximately rep resent 3 axis motion by three SISO systems.

$$m\ddot{x}_{G2} = -3(\mathrm{k_s} + \mathrm{k_L})x_{G2} - 3c_s\dot{x}_{G2} + k_L e_x \quad (2)$$

$$m\ddot{y}_{G2} = -3(\mathrm{k_s} + \mathrm{k_L})y_{G2} - 3c_s\dot{y}_{G2} + k_L e_y \quad (3)$$

$$I\ddot{\theta}_{G2} = \frac{-3(\mathrm{k_s} + \mathrm{k_L})r^2}{2}\theta_{G2} - \frac{3}{2}c_s r^2\dot{\theta}_{G2} + k_L r e_\theta \quad (4)$$

The behavior of the outputs of x_{G2}, y_{G2}, and θ_{G2} for the inputs o

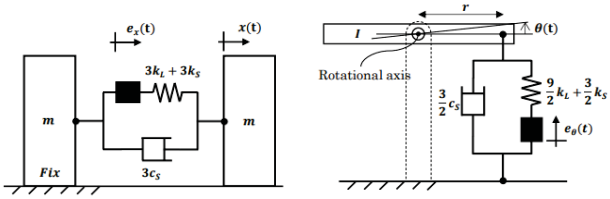

Fig. 3 Single axis model

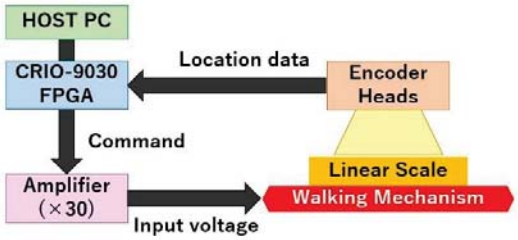

Fig. 4 Measurement system

f e_x, e_y, and e_θ are combined by transfer functions of $P_x(s)$, $P_y(s)$, $P_\theta(s)$ of the second-order delay system.

$$P_x(s) = \frac{k_L}{ms^2 + 3c_S s + 3(k_S + k_L)} \quad (5)$$

$$P_y(s) = \frac{k_L}{ms^2 + 3c_S s + 3(k_S + k_L)} \quad (6)$$

$$P_\theta(s) = \frac{2rk_L}{2Is^2 + 3r^2 c_S s + 3r^2(k_S + k_L)} \quad (7)$$

4. Experiment setup

Fig. 4 shows a schematic diagram of the experimental setup. LabVIEW was used to drive the mechanism and to measure its movement by counting TTL signals from four encoders. The control signals are generated by FPGA. Then, those signals are amplified 30 times by an amplifier before they are inputted to PAs. Optical encoders were used to measure XYθ displacement. The TTL signals are returned to the FPGA to calculate the measurement. The measurement period of this experimental setup is less than 0.1 [ms], which is sufficient for the measurement of the mechanism, whose natural frequency is less than 1000 [Hz].

5. Comparison of 3 control methods

5.1 BangBang control experiments

Fig. 5 shows the results of the BangBang control of the movable leg. In this case, the acceleration was limited so that the fixed leg does n't slip due to inertia. The experiment was conducted 11 times. In In F ig. 5, the black line is ideal trajectory, the red line is that with the mini mum convergence value, and the purple line is that with the maximu m convergence value. Both trajectories reached about ±1% of the targ et value within 20[ms]. They were settled around 100[ms]. The residu al deviations were about 0.2 [μm]. The targeted accuracy of ±0.1[μm] have not been achieved.

BangBang control applies only a predetermined value of voltage. The variation in the convergence value at each session may be due to the friction between the movable leg and the floor surface. Especially right after the start of the positioning, the actual trajectory has a slower rise time than that of the ideal trajectory by the static frictional force. We plan to include the friction forces in the mechanical model for improving the input voltage of BangBang control. The vibration of about 300~500 [Hz] was observed which are around the resonant frequency.

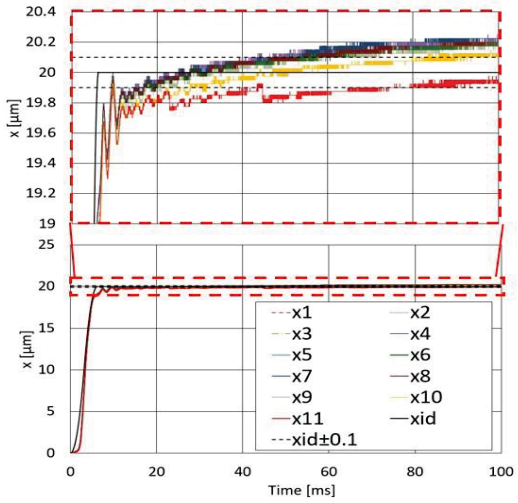

Fig. 5 Plots of X vs. time of BangBang control experiments

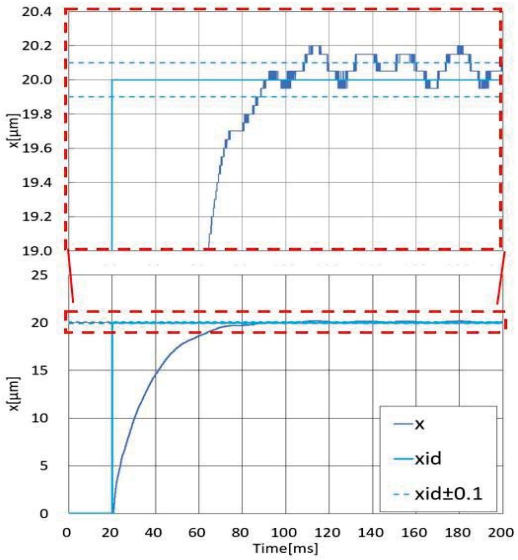

Fig. 6 Plots of X vs. time of PID control experiments

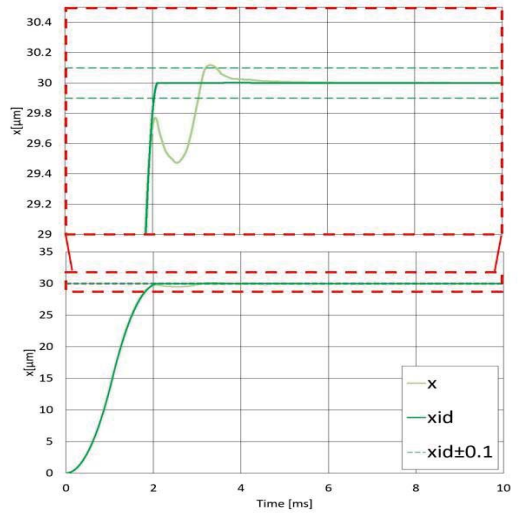

Fig. 7 Plots of X vs. time of simulation of switching control of BangBang and PID controls

5.2 PID control experiments

Main reason for conducting PID control is to remove the residual deviation. The target value was given as a step waveform of 10 [μm] in the x direction, and experiments were conducted five times. The results of each of the five experiments were similar properties, so that we concluded that the repeatability of the mechanical behavior was sufficient. Fig. 6 shows one of the typical experimental results. The residual deviation was within ±0.2 [μm] of the target value ~~without overshooting~~. There were no significant fluctuations in the y- and θ-directions. The oscillation in X axis were observed even after 100 [ms], when Y and θ displacements were converged within corresponding thresholds.

The following four points might be the main reasons for the residual vibration. The first possible reason is an electrical noise which was influenced only in X axis signal. The second point is that the PID gain was obtained by trial and error. A method for determining a reasonable PID gain should be considered. Second, the cutoff frequency of the pseudo-differential low-pass filter used in D control, 50 [Hz], was much lower than the resonance frequency of the mechanism, 450 [Hz]; the cutoff frequency of 50 [Hz] eliminating the residual vibration around 450 [Hz] before D controller. Forth, the fixed leg may have slipped; the more deviation, the higher the output due to the specification of PID control. It is possible that the output is so large that the inertia force exceeds the frictional force between the stationary legs and the floor surface.

5.3 BangBang to PID switching simulation

Fig. 7 shows a MATLAB simulation of the switching control from BangBang to PID control. From the aforementioned result, we considered that if fine adjustment was performed by PID control after rough positioning by BangBang control, both shortening of settling time and elimination of residual deviation could be achieved. When switching control methods, the PID gains were smoothly changed according to a sigmoid function with a time interval of 1 [ms]. White noise was used as sum of the modeling errors and disturbances. As a result, no residual deviations were observed, and the target value was settled within ±0.1 [μm] in approximately 3.5 [ms]. Because those are sufficient for the targeted performances, we concluded that the proposed method is feasible for fast and precise control of the step motion of the robot.

In this simulation, we were not considered the friction between the movable leg and the floor surface, parameter variations due to assembly errors, and hysteresis characteristics of PAs. Thus, in actual experiment, it is expected to take more time to settle.

6. Conclusions

This paper's objective was to improve the accuracy of the motion within a single step of the piezoelectric driven walking mechanism. The targeted accuracy is ±0.1 [μm]. The targeted settling time should have been less than 10 [ms].

In experiments of BangBang control, the robot roughly positio ns the leg, however it caused a residual deviation of up to 0.2[μm] from the target value of 20[μm].

In experiments of PID control, the leg settles within 20±0.1 [μm] of the targeted value without overshooting and eliminates residual deviation.

In simulation of proposed method of switching to PID control after BangBang control, we evaluated that there is feasibility for reducing settling time down to 3.5 [ms] and eliminating the residual deviation within ±0.1 [μm].

We are now constructing the experimental setup for checking the actual behavior of the proposed method. We plan to improve the dynamic model for including the hysteresis characteristics of PAs and the static and kinematic frictional conditions so that the settling time of BangBang control decreases down to 10[ms].

ACKNOWLEDGEMENT

This research was partially supported by the Research Foundation for Electrotechnology of Chubu in FY 2009 and by Grant-in-Aid for Scientific Research (C) (Issue No. 16K06178) in FY 2008. We thank them for their generous support.

REFERENCES

1. J. Kim, An. Banks et al., "Miniaturized Flexible Electronic Sy stems with Wireless Power and Near-Field Communication Ca pabilities", Adv. Funct. Mater., 25, 4761–4767, 2015
2. Itaki, T., Taira, Y., Kuwamori, N. *et al.* Automated collection of single species of microfossils using a deep learning–micromanipulator system. *Prog Earth Planet Sci* **7,** 19 (2020).
3. Hamed tavakoli, Wan Zhou, Lei Ma, Stefani Perez, Andre Ibarra, Feng Xu, Shui Zhan, Xiujun Li, “Recent advances in microfluidic platforms for single-cell analysis in cancer biology, diagnosis and therapy”, Trends in Analytical Chemistry (TrAC), Volume 117, August 2019, pages 13-26
4. Roel J. E. Merry, Niels C. T. de Kleijn, Marinus J. G. van de Molengraft, and Maarten Steinbuch, Senior Member, “Using a Walking Piezo Actuator to Drive and Control a High-Precision Stage”, IEEE/ASME TRANSACTIONS ON MECHATRONICS, vol. 14, no. 1, February 2009
5. Wei Gao, Shinji Sato, Yoshikazu Arai, “A linear-rotary stage for precision positioning”, Precision Engineering 34, 2010, p p.301-306
6. Chien-Sheng Liu, Jie-Yu Zeng&Yu-Ta Chen, “Development o f positioning error measurement system based on geometric optics for long linear stage”, The International Journal of Ad vanced Manufacturing Technology 115, 2595-2606(2021)
7. Qi Su, Qiquan Quan, Jie Deng and Hongpeng Yu, “A Quadruped Micro-Robot Based on Piezoelectric Driving”, Sensors 2018, 18, 810; doi:10.3390/s180303810
8. F. Shono, N. Mouri, T. Higuchi and O. Fuchiwaki, "Simulation of 3-axis state feedback controller with bang-bang control for positioning mechanism driven by 6 piezoelectric actuators," 2016 IEEE International Conference on Advanced Intelligent Mechatronics (AIM), 2016, pp. 1533-1538
9. K. Tanabe, S. Masato, K. Eiji and F. Ohmi, "Precise trajectory measurement of self-propelled mechanism by XYθ three-axis displacement sensor consisting of multiple optical encoders," 2021 60th Annual Conference of the Society of Instrument and Control Engineers of Japan (SICE), 2021, pp. 1001-1006.
10. M. Yatsurugi et al., Modeling and primary experiment of a 3-axis PID control with 50nm resolution for a holonomic precision inchworm robot, ICRA2014, pp. 2552-2558, 2014